Theory of stochastic resonance for small signals in weakly-damped bistable oscillators

P. S. Landa[1,2], I. A. Khovanov[2], and P. V. E. McClintock[2]
[1]*Physics Department, Lomonosov Moscow State University, Moscow 119899, Russia and*
[2]*Department of Physics, Lancaster University, Lancaster LA1 4YB, UK*

The response of a weakly-damped bistable oscillator to an external periodic force is considered theoretically. In the approximation of weak signals we can write a linearized equation for the signal and the corresponding nonlinear equation for the noise. These equations contain two unknown parameters: an effective stiffness and an additional damping factor. In the case of the weakly-damped bistable oscillator, considered here, the two-dimensional Fokker–Planck equation corresponding to the equation for the noise can be solved approximately by changing to a slow variable ("energy") and applying a method of successive approximation. This approach allows us to find the unknown parameters and to calculate the amplitude ratio of the output and input signals, i.e. the gain factor.

PACS numbers: 05.40.-a 05.10.Gg 02.50.-r
Keywords: Stochastic resonance, weakly-damped bistable oscillator, noise, Fokker-Planck equation

INTRODUCTION

In the last three decades a plethora of works has been devoted to studies of *stochastic resonance* (SR). The notion of SR was first introduced [1–3] in an attempt to understand the Earth's ice-age cycle. By this term, the authors of these and other works imply the presence in the system under consideration of a resonance-like nonmonotonic dependence on noise intensity of the system's response to a weak harmonic signal. For the most part this "resonance" has little in common with classical resonance observed in a system when some of its frequencies coincide or become multiples of each other.

There is, however, no precise generally accepted definition of SR. Some authors use the requirement of a noise-induced increase in the signal-to-noise *ratio* at the output. Others restrict the term to describe manifestations of the phenomenon in bistable systems. Moreover, preferred explanations of SR tend to be somewhat individual. SR has a prehistory as well as a history and a very active present, with a huge international activity and applications appearing in almost every area of science. Given the extensive reviews of SR [4–6] and Ch. 14 in [7] we will restrict ourselves to a few succinct introductory remarks to set the context of the present paper.

SR was observed in bistable electronic circuits [11–13], in a ring-laser [14], and then in numerous other systems in both the physical and biological sciences; new applications are frequently reported. Recently a phenomenon similar to stochastic resonance was discovered experimentally in acoustically-excited, turbulent, submerged jets [15], where the role of noise is played by turbulence. Originally, SR seemed a rather mysterious phenomenon, and it was assumed to be restricted to the overdamped bistable systems in which it had been discovered. Many theories of SR, valid under particular circumstances, were proposed [5]. However, it was the realization [16] that SR could be described by linear response theory (LRT) that enabled the phenomenon to be set squarely in the context of earlier research in statistical physics and led to the appreciation [4] that rather similar concepts had been developed by Debye [17] more than half a century earlier, which may be considered as the "prehistory" of SR. More importantly, LRT enlarged the range of occurrence of SR to encompass all systems characterized by strongly noise-dependent susceptibilities, and the requirement of bistability then disappeared. The LRT approach has been validated on bistable [16, 18, 19] and monostable [20] systems in the limit of a extremely weak signals when thermal equilibrium can be assumed and the susceptibility can be obtained from the fluctuation dissipation theorem, as well as in highly nonequilibrium systems [21, 22] where the susceptibility must be obtained in other ways. Thus the LRT approximation illuminates very well the essential physics underlying SR. However, it does not necessarily provide the best way of calculating accurately the signal enhancement to be anticipated under any given conditions (see [7, 23] for discussions).

In what follows we propose a different theoretical approach and we show that it is capable, in principle, of providing whatever level of accuracy may be required. It is based on the idea [7] that the influence of noise on a nonlinear system may be quantified in terms of the resultant change in the effective parameters of the system. This general approach is applicable, not only to SR in the archetypal overdamped bistable system [23–25], but also to the SR that arises in weakly-damped (underdamped) bistable oscillators [7]. Note that the general approach is not restricted to the SR configuration, and it can be applied for the analysis a wide class of weak damped nonautonomous systems. We develop a theoretical description of SR in weakly-damped oscillators by using this approach. The idea underlying our new approach is similar to that developed in mechanics for systems subject to fast vibrations [8]. In the latter work, it was shown that fast vibration changes the system's parameters with respect to slow (averaged) motions. For the calculation of these parameters, the initial equations of the system were broken into two parts: for fast and slow motion respectively. In a very similar way, we split our initial equation into two equations: an averaged equation for the signal, and a stochastic equation for the noise. These equations contain two unknown parameters – an effective stiffness and an effective damping factor, which are expressed in terms of the third moment of the probability distribution. By calculating this moment, we can in turn calculate these unknown parameters. Note that the scheme differs from that used to describe the vibrational resonance in bistable system [9] and diffusion on a vibrated substrate [10]. In the latter cases averaging over the fast periodic force was used.

SR has been demonstrated in weakly-damped bistable oscillators and studied extensively, both experimentally and theoretically [26–29]. It was shown experimentally [28] that, in some parameter regions, a double-peaked structure appears in the dependence of the gain factor on noise intensity. It is observed for small damping and within a frequency range close to the deterministic natural frequency of small oscillations. Alfonsi et al [28] explained the double-peaked structure in terms of the coexistence/competition of intrawell SR of monostable systems [31], and the conventional interwell SR seen in overdamped bistable oscillators. Some matching conditions between the signal frequency and the introduced noise-dependent frequencies were used for the explanation of both peaks [28]. To describe the double structure analytically, the method of moments was considered [29] with a linear response background. Although the method provides a satisfactory description, the authors stressed the poor convergence of the method for weak damping and the necessity of using a large number of moments [29]. However our numerous calculations have shown that the method of moments as applied to SR problem diverges, although it can work for other even more complex problems, see for example [30]. In addition to intra- and interwell motions, used for the explanation in [28], Kang et al [29] considered vibrations over the barrier to explain the double-peaked structure. Note that the explanations cannot be considered adequate since, for example, the frequency matching conditions used do not hold, as we show below. In this paper, too, we consider analytically the case of double-peak structure. We show below that the additional damping factor plays a crucial role in the appearance of the two peaks. This follows from the fact that, in the first approximation giving satisfactory agreement with numerical calculation with respect to effective stiffness, two peaks are not obtained.

In Sec. I we present the results of numerical simulations of SR and a comparison of different approaches. Our analytic technique for calculation of the system response using the effective parameters approach with a linearized equation is presented in the Sec. II, but the associated technical details are provided in the Appendix. Different orders of approximation are discussed in Sec. III and the conclusions drawn are summarized in Sec. IV.

I. THE MODEL AND NUMERICAL RESULTS

Let us consider a weakly-damped bistable oscillator described by the equation

$$\ddot{x} + 2\delta\dot{x} - x + x^3 = A\cos\omega t + \sqrt{K}\xi(t), \qquad (1)$$

where $\xi(t)$ is white noise of intensity K, and $\delta \sim K \ll 1$ is a damping factor. One example of such an oscillator is a pendulum placed between the opposite poles of a magnet. The parameters $\delta = 0.1$, $A = 0.1$ and $\omega = 1$ are selected from the range within which the gain displays the double-peaked structure. Note that its presence does not depend on A (within the validity of theory) but is defined by δ and ω (see below). The noise intensity K is chosen as the adjustable parameter for consideration. We emphasize that, for the selected parameter values, inter-state transitions of the bistable oscillator do not occur in the absence of noise.

For completeness of the presentation, numerical simulations of the Langevin equation (1) were performed and the power spectrum $P(\Omega)$ for the system output $x(t)$ and for the input signal $A\cos\omega t + \sqrt{K}\xi(t)$ were calculated. Additionally the two-state approximation [5] was used to calculate the mean switching frequency $\langle w\rangle$ between the states of the oscillator. The variable $x(t)$ was therefore filtered by a symmetrical trigger with thresholds $\Delta = \pm 0.5$ to produce a dichotomous (two-state) signal $x_f(t)$ confined to the values $\pm|x_m|$ only; here $x_m = \pm 1$ are the coordinates of the stable states of (1). Calculating the mean number of sign changes of $x_f(t)$ during unit time interval we could estimate $\langle w\rangle$.

It should be noted that we have used a non-standard technique for numerical calculations of the parameters interesting for us from Eq. (1). This technique is described in [7]. Usually the calculations of such parameters are based on the analysis of power spectra of $x(t)$ in which, as known, discrete components at the signal frequency ω must be present. It is very difficult to calculate from these spectra the ratio between the amplitudes of output and input signal (the gain factor Q) and the phase shift ψ. Our technique is based on the principle of the so-called synchronous detector. It consists in the following. We calculate the sine B_s and cosine B_c components of the output signal by way of average over a large time:

$$B_s = \frac{2}{nT}\int_0^{nT} x(t)\sin\omega t\,dt,$$

$$B_c = \frac{2}{nT}\int_0^{nT} x(t)\cos\omega t\,dt,$$

where $T = 2\pi/\omega$ and n is a large integer. It is evident that

$$Q = \sqrt{B_s^2 + B_c^2}\,, \quad \psi = \arctan\frac{B_s}{B_c}\,. \qquad (2)$$

The output signal component for $x_f(t)$ and the gain factor Q for the two state filter were defined in similar ways.

Using the power spectra of $x(t)$, $x_f(t)$ and the input signal we calculate the signal-to-noise ratio R following the standard definition [5, 32]. The signal-to-noise ratio is defined as the common logarithm of the power ratio between the signal, S_i^2, and noise, P_n, components

$$R = 10\log_{10}\frac{S_i^2}{P_n}. \tag{3}$$

By definition, R is measured in decibel (dB) units. Following [5] the noise component was estimated using the power spectrum $P(\Omega)$ of the output signal $x(t)$ (or $x_f(t)$) in the following way

$$P_n = \Delta\Omega\frac{1}{2m}\left[\sum_{j=i-m, j\neq i}^{j=i+m} P(\Omega_j)\right], \tag{4}$$

where $\Delta\Omega$ is the frequency resolution in the numerically calculated power spectrum $P(\Omega)$; $\Omega_i = \omega$ and $m = 10$ defines a bandwidth to approximate the noise component at signal frequency ω [33]. The input R was included to verify the results of numerical simulations, since the input R can be calculated directly as $R = 10\log_{10}\frac{A^2}{K\Delta\Omega}$.

Fig. 1 collects the results of numerical simulations. The SR effect manifests in the dependence of the gain factor Q on K as the presence of two maximal values, whereas the signal-to-noise ratio, calculated for the full dynamics of $x(t)$, demonstrates monotonic decay without any extremum as shown by the full (green) line in Fig. 1(a). However R, calculated by the two-state method [dot-dashed (blue) line in Fig. 1(a)] reveals SR. There is evidently no correspondence between the behaviors of R and Q. On the other hand the dependence of $\langle\omega\rangle$ on K clearly indicates the absence of a matching condition between the mean switching frequency and the signal frequency for the second maximum of Q. The latter conclusion does not support the explanation of SR presented by Alfonsi et al [28]. Note that the gain factors Q, calculated via both the full dynamics $x(t)$ [the full (green) line in Fig. 1(c)] and the two-state approximation $x_f(t)$ [the dot-dashed (blue) line in Fig. 1(c)], demonstrate similar behavior for large noise intensity.

In addition, Q and ψ were calculated numerically [dashed (red) lines in Fig. 1 (c) and (d)] by linear response theory. In linear response theory (LRT) [16, 17, 27] the time dependent mean value of the system response is determined via the linear susceptibility of the system:

$$\langle x(t)\rangle = A\Re[\chi(\omega)\exp(-i\omega t)] + \text{const}; \tag{5}$$

where A and ω are the amplitude and frequency of the external signal and $\chi(\omega)$ is the linear susceptibility of the system. An important feature of LRT is the fact that the susceptibility is determined *in the absence* of external

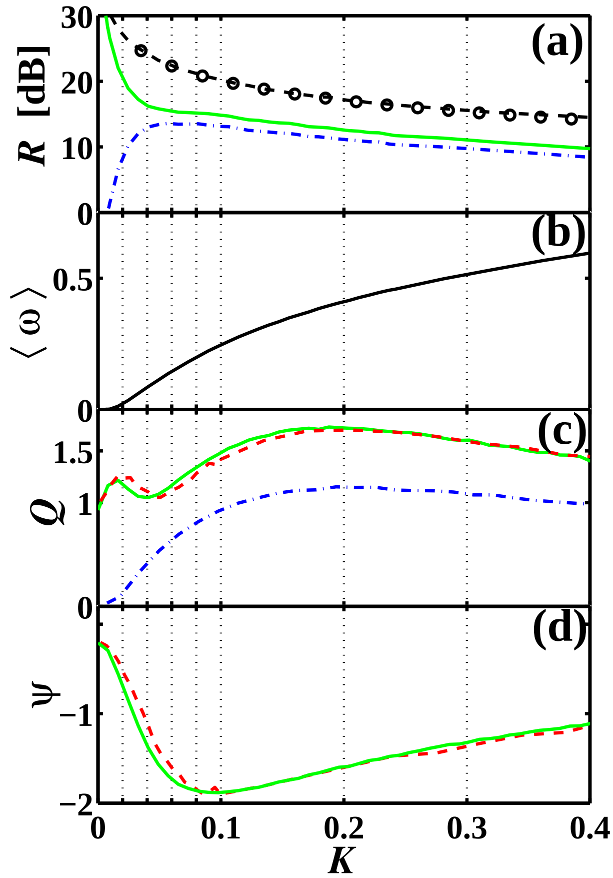

FIG. 1: (Color online) Results of numerical simulations. (a) The signal-to-noise ratio R as a function of noise intensity K. The dashed (black) line corresponds to the input value, calculated numerically, whereas the circles correspond to theoretical values. The full (green) line corresponds to the output R calculated for $x(t)$; the dot-dashed (blue) line was calculated using the two-state approximation. (b) The mean switching frequency $\langle\omega\rangle$ is shown as a function of K. (c) The gain factor Q and (d) the phase shift ψ are shown as functions of noise intensity K. Full (green) lines corresponds to numerical simulations of (1), dashed (red) lines correspond to linear response theory, and dot-dashed (blue) lines correspond to results that were calculated numerically in the two-state approximation.

signal and it has the following relationship to the spectral density $S_0(\Omega)$ of the system when forced only by noise:

$$\Re\chi(\Omega) = \frac{2\delta}{K}\mathrm{P}\int_0^\infty d\omega_1\frac{S_0(\omega_1)\omega_1^2}{(\omega_1^2-\Omega^2)}, \tag{6}$$

$$\Im\chi(\Omega) = \frac{\pi\delta\Omega}{K}S_0(\Omega). \tag{7}$$

The gain factor Q and the phase shift ψ are defined by the following relations via the susceptibility:

$$Q = |\chi(\Omega)|, \tag{8}$$

$$\psi = -\arctan\left[\frac{\Im\chi(\Omega)}{\Re\chi(\Omega)}\right]. \tag{9}$$

The spectral density $S_0(\Omega)$ was calculated by numerical simulation of the Langevin equation (1) for $A = 0$ and then the equations (8) and (9) were used to determine Q and ψ. The results [dashed (red) lines in Fig. 1 (c) and (d)] demonstrate the applicability of LRT.

Now let us turn to the analytic consideration of the problem. We use a weak signal approximation that allows us to arrive at a linear equation for the signal and a nonlinear equation for the noise. Note that, although the idea of LRT looks very similar to the linearization technique presented below, they are in fact fundamentally different approaches as it will be clear from what follows.

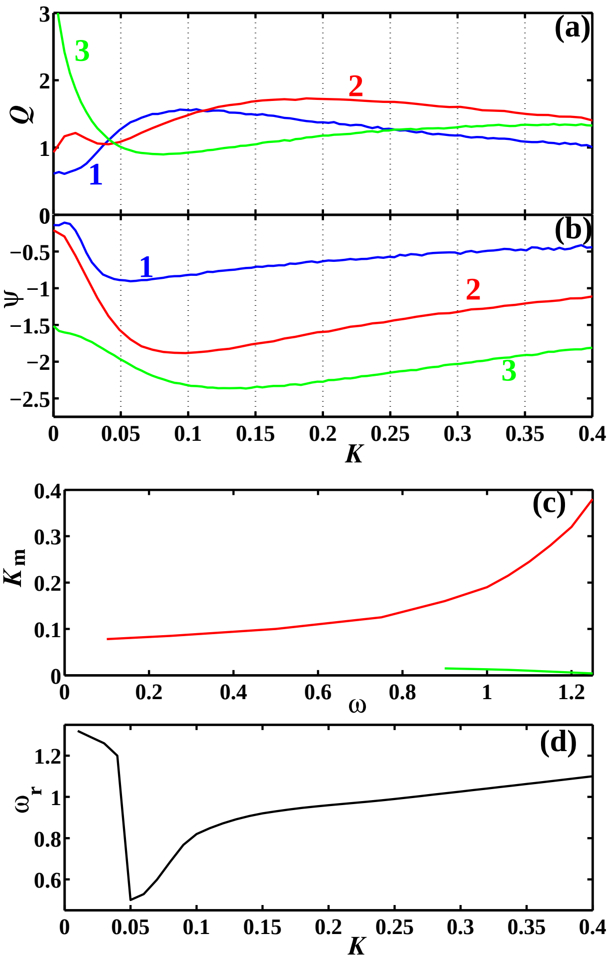

FIG. 2: (Color online) The dependences of the gain factor Q (a) and phase shift ψ (b) on the noise intensity K for $\delta = 0.1$, $A = 0.1$ and $\omega = 0.5$, $\omega = 1$, and $\omega = 1.25$ (curves 1 (blue), 2 (red) and 3 (green), respectively); (c) the plot of K_m versus ω for maximum of Q; (d) the numerical dependence of the resonant frequency ω_r on K.

The output of system (1) consists [34] of two components. One corresponds to the external signal and is periodic function of time; and the other is the noisy part. Let us denote the signal part as $s(t)$ and noisy as $n(t)$. In the weak signal approximation the signal part of the output can be presented (see details below) as the response of deterministic linear system:

$$\ddot{s} + (2\delta + b)\dot{s} + cs = A\cos\omega t, \tag{10}$$

where $2\delta + b$ and c are an effective damping and effective stiffness (by analogy with the stiffness of a linear spring) respectively. They are determined by both the signal part s and the noise n. The effective damping consists on an initial system damping 2δ and additional term b. This representation allows us to use a simplified description in terms of the response of a linear oscillator, and it introduces a natural frequency of the system (10) and, consequently, of the system (1).

The noise-induced changes in the effective stiffness and damping factor result in a corresponding change in the effective natural frequency. It follows that the response of such an oscillator to the input signal $A\cos\omega t$ is dependent on the noise intensity and the system parameters. Numerical simulations of Eq. (1) have confirmed that this is indeed the case. As shown in Fig. 2 (a) and (b), the gain factor Q and the phase shift ψ depend significantly on the signal frequency ω. For $\omega = 0.5$ the dependences are close to the case of an overdamped oscillator [23, 24], whereas for larger frequencies they differ markedly. The double peaked structure in Q vs K is only observed within a specific frequency range: within a certain range of ω close to the oscillator's natural frequency for small oscillations, these dependences have two maxima. The first maximum is observed for small, and the second maximum for large, noise intensities. For the second maximum the dependence on ω of the noise intensity K_m [Fig. 2(c)] corresponding to the maximum of Q is similar to that for an overdamped oscillator. Whereas for the first maximum (located at small K), the value of K_m *decreases* as ω increases. The first maximum is caused by a resonance-like moderate change of the noise-induced additional damping factor, whereas the second maximum is caused by an abrupt change in oscillation frequency associated with the onset of interwell transitions. The first maximum appears when the noise intensity and signal amplitude are such that the effective natural frequency of small oscillations becomes equal to the signal frequency.

In contrast to the overdamped oscillator [23, 24], the dependences of Q on ω are of a resonant character, with a resonant frequency ω_r depending on K [see Fig. 2(d)]: as K increases, ω_r at first decreases abruptly, and then increases slowly. Such behavior of the resonant frequency is attributable to the nonmonotonic change in effective stiffness and damping factor with K. The fact that the resonant frequency of a nonlinear oscillator may be controlled by external noise is of potential importance in practical applications.

Starting from calculated numerically values of Q and ψ we can calculate the effective stiffness c, the addition b to the damping factor and the effective natural frequency

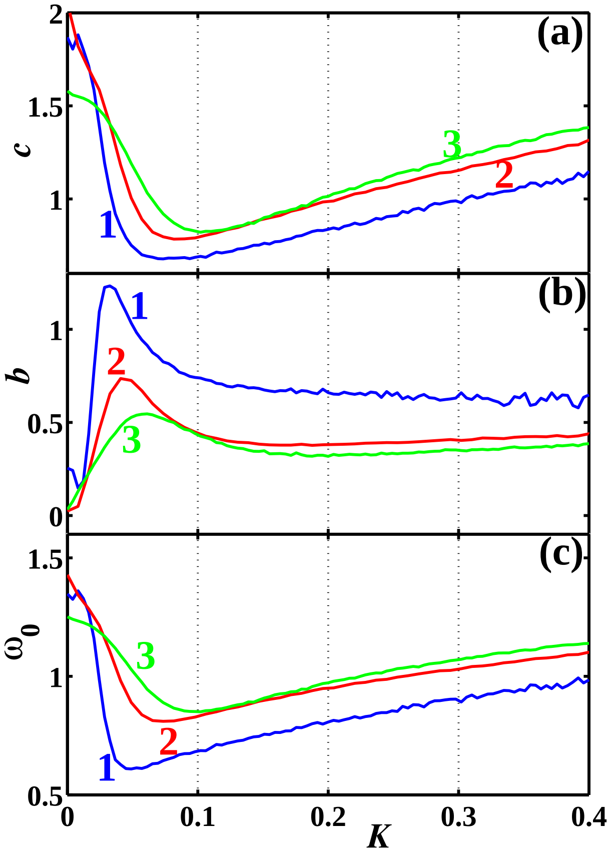

FIG. 3: (Color online) The dependences on noise intensity K of (a) the effective stiffness c, (b) the addition b to the damping factor and (c) the natural frequency ω_0, for $\delta = 0.1$, $A = 0.1$ and $\omega = 0.5$, $\omega = 1$, and $\omega = 1.25$ (curves 1 (blue), 2 (red) and 3 (green), respectively).

ω_0 by use of the equations

$$\begin{aligned} c &= \omega^2 + \frac{\cos\psi}{Q}, \\ b &= -\left(2\delta + \frac{\sin\psi}{\omega Q}\right), \\ \omega_0 &= \sqrt{c - \left(\delta + \frac{b}{2}\right)^2}. \end{aligned} \tag{11}$$

The calculated dependences of c, b and ω_0 on K are illustrated in Fig. 3 for $A = 0.1$ and the same frequencies as in Fig. 2(a) and (b). Comparing the dependence of the effective natural frequency ω_0 with the resonant frequency [7] we can see that they are somewhat different.

These results clearly demonstrate significant dependence of Q and ψ on both the noise and the signal parameters. Consequently, any real information-carrying signal will be significantly distorted, so that and SR is not an appropriate way to amplify such signals. However, SR is very effective for the task of signal determination, e.g. in computer tomography or to locate submarines.

II. DEVELOPMENT OF THE THEORY

For the sake of convenience we introduce a conditional small parameter ϵ and rewrite Eq. (1) as

$$\ddot{x} + 2\epsilon\tilde{\delta}\dot{x} - x + x^3 = A\cos\omega t + \sqrt{\epsilon\tilde{K}}\xi(t), \tag{12}$$

To solve the problem analytically, we write the solution of Eq. (12) as

$$x(t) = s(t) + n(t), \tag{13}$$

where $s(t) = \langle x(t)\rangle$ and n is the deviation from this mean value. As in earlier work [7, 23, 24] we separate Eq. (12) into two equations, one describing quantities averaged over the statistical ensemble, and the other describing deviations from the averaged values. In so doing we take into account that the third moment $m_3 = \langle n^3\rangle$ depends on the signal $s(t)$. In the linear approximation with respect to s we can set $m_3 = as + \epsilon b\dot{s}$, where a and b are unknown parameters. To the same approximation, the equations for s and n are

$$\ddot{s} + \epsilon(2\delta + b)\dot{s} + cs = A\cos\omega t, \tag{14}$$

$$\begin{aligned} \ddot{n} - n + n^3 + (3n^2 - 1 &- c)s \\ -\epsilon b\dot{s} + 2\epsilon\delta\dot{n} &= \sqrt{\epsilon}\xi(t), \end{aligned} \tag{15}$$

where $c = 3m_2 - 1 + a$ can be treated as an effective stiffness, b is the addition to damping factor δ, and $m_2 = \langle n^2\rangle$. It follows from Eq. (14) that

$$s(t) = AQ(\omega)\cos\Big(\omega t + \psi(\omega)\Big), \tag{16}$$

where

$$\begin{aligned} Q(\omega) &= \frac{1}{\sqrt{(c-\omega^2)^2 + \epsilon^2(2\delta + b)^2\omega^2}}, \\ \cos\psi(\omega) &= (c - \omega^2)Q(\omega), \\ \sin\psi(\omega) &= -\epsilon(2\delta + b)\omega Q(\omega). \end{aligned} \tag{17}$$

It is thus evident that, if we know c and b, we can calculate the gain factor $Q(\omega)$ and phase shift $\psi(\omega)$.

As shown by Stratonovich [35], for small ϵ it is convenient to introduce the "energy" E, which is a slow variable, in place of the fast variable $\dot{n}$. Such a change of variables allows us to find e.g. the exact solution of the Fokker–Planck equation in the absence of the signal. To do this, we set

$$E = u(n) + \frac{\dot{n}^2}{2}, \tag{18}$$

where $u(n) = n^4/4 - n^2/2$ is the bistable potential. Multiplying Eq. (15) by $\dot{n}$ and taking account of (18) we obtain two Langevin equations for variables n and E:

$$\dot{n} = \sqrt{2\Big(E-u(n)\Big)},$$
$$\dot{E} = -\sqrt{2\Big(E-u(n)\Big)}\Big[(3n^2-c-1)s-b\dot{s}\Big]-4\epsilon\delta\Big(E-u(n)\Big)+\sqrt{2\epsilon\Big(E-u(n)\Big)}\xi(t). \tag{19}$$

It is evident that the solution of Eqs. (19) is real only for $E \geq u(n)$. It follows that $E \geq -1/4$ and $\alpha(E) \leq |n| \leq n_2(E)$, where

$$\alpha(E) = \begin{cases} n_1(E) & \text{for } -1/4 \leq E \leq 0, \\ 0 & \text{for } E \geq 0, \end{cases} \qquad n_{1,2}(E) = \sqrt{1 \mp \sqrt{1+4E}}\,. \tag{20}$$

Taking account of the dependence of noise intensity on E, the Fokker–Planck equation for the probability density $w(n,E,t)$ is

$$\frac{\partial w}{\partial t} = -\frac{\partial}{\partial n}\left(\sqrt{2\Big(E-u(n)\Big)}\,w\right)+\frac{\partial}{\partial E}\left\{\left[\sqrt{2\Big(E-u(n)\Big)}\Big[(3n^2-c-1)s-b\dot{s}(t)\Big]\right.\right.$$
$$\left.\left. +\ 4\epsilon\delta\Big(E-u(n)\Big)-\epsilon\,\frac{K}{2}\right]w+\epsilon K\,\frac{\partial}{\partial E}\Big[\Big(E-u(n)\Big)w\Big]\right\}. \tag{21}$$

Because of the linearity of Eq. (21), we can represent its steady-state solution as a sum of three components

$$w(t,n,E) = w_0(n,E)+w_1(n,E)s(t)+\frac{w_2(n,E)\dot{s}(t)}{\omega}\,. \tag{22}$$

From the normalization condition for $w(t,n,E)$ we obtain the following conditions:

$$2\int\limits_{-0.25}^{\infty}\int\limits_{\alpha(E)}^{n_2(E)} w_0(n,E)\,dn\,dE = 1, \tag{23}$$

$$\int\limits_{-0.25}^{\infty}\int\limits_{\alpha(E)}^{n_2(E)} w_{1,2}^{(e)}(n,E)\,dn\,dE = 0, \tag{24}$$

where $w_{1,2}^{(e)}(n,E)$ are even components of the functions $w_{1,2}(n,E)$.

For a small harmonic signal s of frequency ω, we take the linear approximation $\ddot{s} = -\omega^2 s$. The equations for $w_0(n,E)$, $w_1(n,E)$ and $w_2(n,E)$ are then

$$\frac{\partial}{\partial n}\left(\sqrt{2\Big(E-u(n)\Big)}\,w_0\right) = \epsilon\,\frac{\partial}{\partial E}\left\{\left[4\delta\Big(E\ -\ u(n)\Big)-\frac{K}{2}\right]w_0+K\,\frac{\partial}{\partial E}\Big[\Big(E-u(n)\Big)w_0\Big]\right\},$$
$$-\omega w_2(n,E)+\frac{\partial}{\partial n}\left(\sqrt{2\Big(E-u(n)\Big)}\,w_1(n,E)\right) - \epsilon\,\frac{\partial}{\partial E}\left\{\left[4\delta\Big(E-u(n)\Big)-\frac{K}{2}\right]w_1(n,E)\right.$$
$$\left.+K\,\frac{\partial}{\partial E}\Big[\Big(E-u(n)\Big)w_1(n,E)\Big]\right\} = (3n^2-c-1)\,\frac{\partial}{\partial E}\left[\sqrt{2\Big(E-u(n)\Big)}w_0(n,E)\right],$$
$$\omega w_1(n,E)+\frac{\partial}{\partial n}\left(\sqrt{2\Big(E-u(n)\Big)}\,w_2(n,E)\right) - \epsilon\,\frac{\partial}{\partial E}\left\{\left[4\delta\Big(E-u(n)\Big)-\frac{K}{2}\right]w_2(n,E)\right.$$
$$\left.+K\,\frac{\partial}{\partial E}\Big[\Big(E-u(n)\Big)w_2(n,E)\Big]\right\} = -\omega b\,\frac{\partial}{\partial E}\left[\sqrt{2\Big(E-u(n)\Big)}w_0(n,E)\right]. \tag{25}$$

By direct substitution into Eq. (25) we can check that its exact solution is

$$w_0(n,E) = \frac{W_0(E)}{\sqrt{2\Big(E-u(n)\Big)}}\,, \tag{26}$$

where

$$W_0(E) = C_0 \exp\left(-\frac{4\delta}{K}\,E\right), \qquad (27)$$

and C_0 is the normalization constant which can be found from the condition (23). Integrating (26) over E from $u(n)$ to infinity we find

$$w_0(n) = \frac{C_0}{2}\sqrt{\frac{\pi K}{2\delta}}\exp\left(-\frac{4\delta u(n)}{K}\right). \qquad (28)$$

From (28) it is simple to calculate m_2 as a function of K/δ. It is evident from Fig. 4 that it passes through a minimum at $K \approx 0.085$.

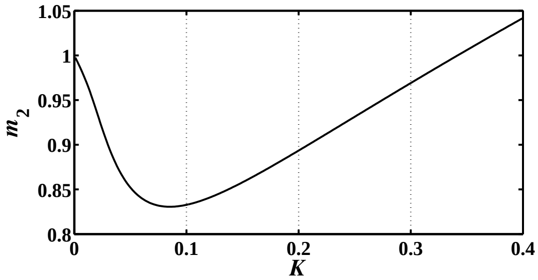

FIG. 4: The dependence of the second moment m_2 on K.

We now seek a solution of Eqs. (25) in the form of a series expansion in terms of ϵ, as

$$\begin{aligned} w_1(n,E) &= w_0(n,E)\Big(w_{10}(n,E) + \epsilon w_{11}(n,E) + \epsilon^2 w_{12}(n,E) + o(\epsilon^3)\Big), \\ w_2(n,E) &= w_0(n,E)\Big(w_{20}(n,E) + \epsilon w_{21}(n,E) + \epsilon^2 w_{22}(n,E) + o(\epsilon^3)\Big), \end{aligned} \qquad (29)$$

where $w_{10}(n,E)$, $w_{20}(n,E)$, $w_{11}(n,E)$, $w_{21}(n,E)$, $w_{12}(n,E)$, $w_{22}(n,E)$, $\ldots$ are all unknown functions. Taking account of the fact that

$$\begin{aligned} &\frac{\partial}{\partial E}\left(2\Big(E-u(n)\Big)w_0(n,E)w_{1j,2j}(n,E)\right) + \left(\frac{8\delta}{K}\Big(E-u(n)\Big)-1\right)w_0(n,E)w_{1j,2j}(n,E) \\ &= W_0(E)\sqrt{2\Big(E-u(n)\Big)}\,\frac{\partial w_{1j,2j}(n,E)}{\partial E} \quad (j=1,2,\ldots), \end{aligned} \qquad (30)$$

and equating coefficients for the same powers of ϵ, for functions $w_{1j}(n,E)$ and $w_{2j}(n,E)$ we obtain the following equations:

$$\frac{\partial w_{10}(n,E)}{\partial n} - \frac{\omega w_{20}(n,E)}{\sqrt{2\Big(E-u(n)\Big)}} = -\frac{4\delta}{K}(3n^2-c-1), \qquad \frac{\partial w_{20}(n,E)}{\partial n} + \frac{\omega w_{10}(n,E)}{\sqrt{2\Big(E-u(n)\Big)}} = \frac{4\delta}{K}\,\omega b, \qquad (31)$$

$$\begin{aligned} &\frac{\partial w_{1j}(n,E)}{\partial n} - \frac{\omega w_{2j}(n,E)}{\sqrt{2\Big(E-u(n)\Big)}} = \frac{K}{2}\left(\frac{\partial}{\partial E} - \frac{4\delta}{K}\right)\left(\sqrt{2\Big(E-u(n)\Big)}\,\frac{\partial w_{1,j-1}(n,E)}{\partial E}\right), \\ &\hspace{20em} \text{for } j=1,2,\ldots \\ &\frac{\partial w_{2j}(n,E)}{\partial n} + \frac{\omega w_{1j}(n,E)}{\sqrt{2\Big(E-u(n)\Big)}} = \frac{K}{2}\left(\frac{\partial}{\partial E} - \frac{4\delta}{K}\right)\left(\sqrt{2\Big(E-u(n)\Big)}\,\frac{\partial w_{2,j-1}(n,E)}{\partial E}\right). \end{aligned} \qquad (32)$$

The stationary solution of Eqs. (31), (32), taken in combination with the normalization condition for the probability density $w(t,n,E)$, the equality to zero of $\langle n\rangle$, and the condition $m_3 = \langle n^3\rangle = as(t) + b\dot{s}(t)$, allow us to calculate the required constants c and b. To find the stationary solution we use the analytic approach outlined below.

It is easy to show that the general solution of the homogeneous equations for given j is

$$w_{1j}^{(\mathrm{h})}(n,E) = C_{1j}\cos\Big(\omega q(n,E)\Big) + C_{2j}\sin\Big(\omega q(n,E)\Big), \quad w_{2j}^{(\mathrm{h})}(n,E) = C_{2j}\cos\Big(\omega q(n,E)\Big) - C_{1j}\sin\Big(\omega q(n,E)\Big), \quad (33)$$

where C_{1j} and C_{2j} are arbitrary constants,

$$q(n,E)=\int\limits_{\alpha(E)}^{n}\frac{dn'}{\sqrt{2\Big(E-u(n')\Big)}}=\begin{cases}\dfrac{\sqrt{2}}{n_2(E)}\,\boldsymbol{F}\Big(g(n,E),k(E)\Big) & \text{for } -1/4<E\le 0,\\ (1+4E)^{-1/4}\,\boldsymbol{F}\Big(g_1(n,E),k_1(E)\Big) & \text{for } E\ge 0,\end{cases}$$

$$k(E)=\frac{\sqrt{2\sqrt{1+4E}}}{n_2(E)}\,,\quad g(n,E)=\sqrt{\frac{n^2-n_1^2(E)}{n^2k^2(E)}}\,,\quad k_1(E)=\frac{1}{k(E)}\,,\quad g_1(n,E)=\frac{1}{g(n,E)}\,, \tag{34}$$

and $\boldsymbol{F}\Big(g(n,E),k(E)\Big)$ is the incomplete elliptic integral of the first kind (see Ch. 17 of [36]). Note that $q(n,E)$ is an odd function of n.

A partial solution of the inhomogeneous Eqs. (31), (32) can be found by a method similar to the well-known method of variation of constants. Accordingly, we seek a solution of these equations as

$$\begin{aligned} w_{1j}^{(\text{in})}(n,E) &= B_{1j}(n,E)\cos\Big(\omega q(n,E)\Big)\\ &+ B_{2j}(n,E)\sin\Big(\omega q(n,E)\Big),\\ w_{2j}^{(\text{in})}(n,E) &= B_{2j}(n,E)\cos\Big(\omega q(n,E)\Big)\\ &- B_{1j}(n,E)\sin\Big(\omega q(n,E)\Big),\end{aligned} \tag{35}$$

where $B_{1j}(n,E)$ and $B_{2j}(n,E)$ are unknown functions. By substituting (35) into Eqs. (31), (32), we find the following equations for these functions:

$$\begin{aligned} &\frac{\partial B_{1j}(n,E)}{\partial n}\cos\Big(\omega q(n,E)\Big)\\ &+\frac{\partial B_{2j}(n,E)}{\partial n}\sin\Big(\omega q(n,E)\Big)=F_{1j}(n,E),\\ &\frac{\partial B_{2j}(n,E)}{\partial n}\cos\Big(\omega q(n,E)\Big)\\ &-\frac{\partial B_{1j}(n,E)}{\partial n}\sin\Big(\omega q(n,E)\Big)=F_{2j}(n,E),\end{aligned} \tag{36}$$

where $F_{1j}(n,E)$ and $F_{2j}(n,E)$ are right-hand members of Eqs. (31), (32). Solving Eqs. (36) we find

$$\begin{aligned} B_{1j}(n,E) &= \int\Big[F_{1j}(n,E)\cos\Big(\omega q(n,E)\Big)\\ &- F_{2j}(n,E)\sin\Big(\omega q(n,E)\Big)\Big]\,dn,\\ B_{2j}(n,E) &= \int\Big[F_{1j}(n,E)\sin\Big(\omega q(n,E)\Big)\\ &+ F_{2j}(n,E)\cos\Big(\omega q(n,E)\Big)\Big]\,dn.\end{aligned} \tag{37}$$

By using these formulae we can solve Eqs. (31), (32) in succession. Technical details of the implementation of the described above technique are presented in the Appendix for zero and first order approximations.

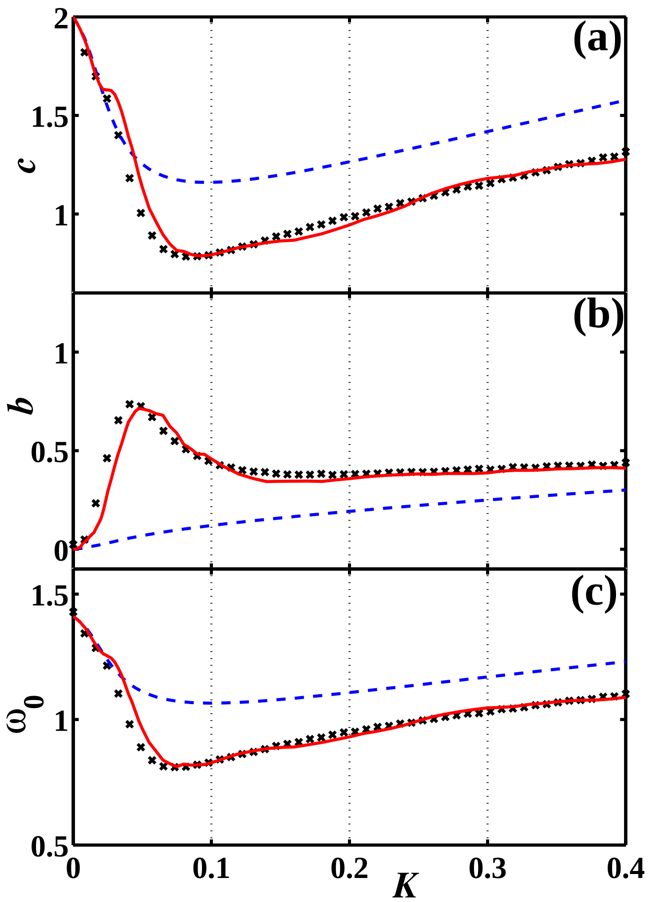

FIG. 5: (Color online) (a) The effective stiffness c, (b) the addition b to the damping factor, and (c) the natural frequency ω_0, are shown as functions of intensity K. Theoretical results in the first and second approximations are shown by dashed (blue) and full (red) lines respectively. The dependences found numerically are shown by crosses.

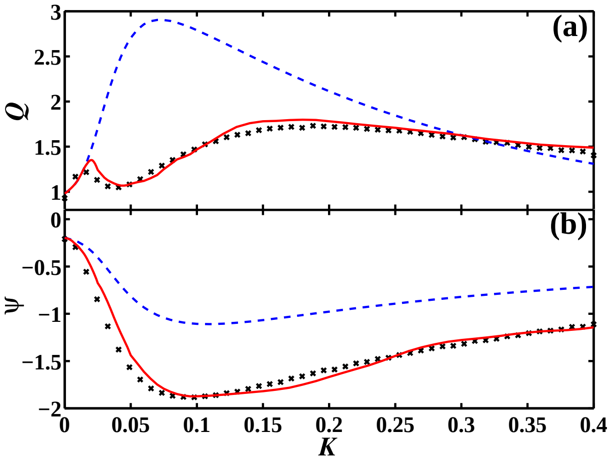

FIG. 6: (Color online) (a) The gain factor Q and (b) the phase shift ψ are shown as functions of noise intensity K. Theoretical results in the first and second approximations are shown by dashed (blue) and full (red) lines respecivelyly. The dependences found numerically are shown by crosses.

III. FIRST VS SECOND ORDER OF APPROXIMATION

The dependences of c, b and ω_0 on K for $\delta = 0.1$ and $\omega = 1$, constructed from the first order approximation are given by the dashed (blue) curves in Fig. 5. The corresponding dependences found from the numerical results presented in [7] are shown by crosses in the same figure. We see that the theoretical dependences differ from those found from numerical calculations. The most significant difference is observed for the additional damping factor b. Apparently, this arises because, in the zeroth approximation with respect to ϵ, $b \equiv 0$ (this means that $b \sim \delta$, i.e. a conservative system cannot become dissipative due to noise), and the higher approximations are necessary to obtain correct results. Fig. 6 illustrates the dependences of the gain factor Q and phase shift ψ on K. These dependences (dashed (blue) lines) also differ from numerical ones, as conditioned the difference in b and c. In particular they do not show two resonances.

The results of the second order approximation are shown in Figs. 5 and 6 by full (red) lines. They are in excellent agreement with the numerical calculations. For most purpose, therefore, it will not be necessary to take the theory beyond the second approximation.

IV. CONCLUSIONS

In summary, we have described a method of calculating the amplitude ratio and phase shift between the input and output signals for a noisy bistable system exhibiting gain due to SR. It is valid in the small-signal limit, which is usually the regime of interest for SR. We tested the results by comparison with numerical simulations. Results calculated in the first approximation are not in good agreement with the numerics, but those in the second approximation are in very good agreement.

The essence of the approach introduced above is the representation of the response to a harmonic signal of a *nonlinear stochastic* system by the response of an effective *linear deterministic* system. The latter is defined by an effective stiffness and an effective damping which depend on the system nonlinearity, the signal parameters and the noise intensity. For the calculation of these parameters, noisy dynamics is considered as a fast motion. It is is averaged to determine the slow motion in terms of the effective stiffness and damping. Consequently the system response can be described in terms that are *natural* for oscillatory systems: stiffness and damping. We believe that the method of effective parameters proposed in this paper provides the most effective way of understanding the mechanism of SR and the best means of calculating the response of the system to an input signal.

Acknowledgements

We are grateful to the Royal Society of London and the Engineering and Physical Sciences Research Council (UK) for their support of this work.

APPENDIX A: APPENDIX

1. Zeroth order approximation

In the zeroth approximation we find

$$\begin{aligned} w_{10}(n,E) &= w_{10}^{(\mathrm{h})}(n,E) + \frac{4\delta}{K}\Big(\omega b I_{20}(n,E) \\ &+ (c+1)I_{10}(n,E) - 3I_{30}(n,E)\Big), \end{aligned} \tag{A1}$$

$$\begin{aligned} w_{20}(n,E) &= w_{20}^{(\mathrm{h})} + \frac{4\delta}{K}\Big(\omega b I_{10}(n,E) \\ &- (c+1)I_{20}(n,E) + 3I_{40}(n,E)\Big), \end{aligned}$$

where

$$I_{10}(n,E) = \int\limits_{n_0}^{n} \cos\Big[\omega\Big(q(n,E) - q(n',E)\Big)\Big]\, dn',$$

$$I_{20}(n,E) = \int\limits_{n_0}^{n} \sin\Big[\omega\Big(q(n,E) - q(n',E)\Big)\Big]\, dn', \tag{A2}$$

$$I_{30}(n,E) = \int\limits_{n_0}^{n} (n')^2 \cos\Big[\omega\Big(q(n,E) - q(n',E)\Big)\Big]\, dn',$$

$$I_{40}(n,E)=\int\limits_{n_0}^{n}(n')^2\sin\Big[\omega\Big(q(n,E)-q(n',E)\Big)\Big]\,dn'.$$

Here, n_0 is an arbitrary number which, for simplicity, we take as unity.

2. First order approximation

In the first approximation

$$\begin{aligned}B_{11}(n,E)&=2\delta\omega\Big(\omega bJ_2(n,E)+(c+1)J_1(n,E)-3J_3(n,E)\Big)\\&-\frac{\omega K}{2}\left[\omega I_{11}(n,E)C_{10}-\left(I_{21}(n,E)-\frac{4\delta}{K}I_{31}(n,E)\right)C_{20}\right],\\B_{21}(n,E)&=2\delta\omega\Big(\omega bJ_1(n,E)-(c+1)J_2(n,E)+3J_4(n,E)\Big)\\&-\frac{\omega K}{2}\left[\omega I_{11}(n,E)C_{20}+\left(I_{21}(n,E)-\frac{4\delta}{K}I_{31}(n,E)\right)C_{10}\right],\end{aligned}\tag{A3}$$

where

$$\begin{aligned}&I_{11}(n,E)=\int\limits_{n_0}^{n}\sqrt{2\Big(E-u(n')\Big)}\left(\frac{\partial q(n',E)}{\partial E}\right)^2dn',\quad I_{31}(n,E)=\int\limits_{n_0}^{n}\sqrt{2\Big(E-u(n')\Big)}\,\frac{\partial q(n',E)}{\partial E}\,dn',\\&I_{21}(n,E)=\int\limits_{n_0}^{n}\left(\sqrt{2\Big(E-u(n')\Big)}\,\frac{\partial^2 q(n',E)}{\partial E^2}+\frac{1}{\sqrt{2\Big(E-u(n')\Big)}}\frac{\partial q(n',E)}{\partial E}\right)dn',\end{aligned}\tag{A4}$$

$$\begin{aligned}&J_1(n,E)=\int\limits_{n_0}^{n}\left(I_{111}(n',E)-\frac{4\delta}{K}I_{112}(n',E)\right)dn',\ J_2(n,E)=\int\limits_{n_0}^{n}\left(I_{211}(n',E)-\frac{4\delta}{K}I_{212}(n',E)\right)dn',\\&J_3(n,E)=\int\limits_{n_0}^{n}\left(I_{311}(n',E)-\frac{4\delta}{K}I_{312}(n',E)\right)dn',\ J_4(n,E)=\int\limits_{n_0}^{n}\left(I_{411}(n',E)-\frac{4\delta}{K}I_{412}(n',E)\right)dn',\end{aligned}\tag{A5}$$

$$\begin{aligned}I_{111}(n,E)=\int\limits_{n_0}^{n}\Bigg\{&\sqrt{2\Big(E-u(n)\Big)}\Bigg[\left(\frac{\partial^2 q(n,E)}{\partial E^2}-\frac{\partial^2 q(n',E)}{\partial E^2}\right)\sin\Big(\omega q(n',E)\Big)-\omega\Bigg(\frac{\partial q(n,E)}{\partial E}\\&-\frac{\partial q(n',E)}{\partial E}\Bigg)^2\cos\Big(\omega q(n',E)\Big)\Bigg]+\frac{1}{\sqrt{2\Big(E-u(n)\Big)}}\left(\frac{\partial q(n,E)}{\partial E}-\frac{\partial q(n',E)}{\partial E}\right)\sin\Big(\omega q(n',E)\Big)\Bigg\}dn',\\I_{211}(n,E)=\int\limits_{n_0}^{n}\Bigg\{&\sqrt{2\Big(E-u(n)\Big)}\Bigg[\left(\frac{\partial^2 q(n,E)}{\partial E^2}-\frac{\partial^2 q(n',E)}{\partial E^2}\right)\cos\Big(\omega q(n',E)\Big)+\omega\Bigg(\frac{\partial q(n,E)}{\partial E}\\&-\frac{\partial q(n',E)}{\partial E}\Bigg)^2\sin\Big(\omega q(n',E)\Big)\Bigg]+\frac{1}{\sqrt{2\Big(E-u(n)\Big)}}\left(\frac{\partial q(n,E)}{\partial E}-\frac{\partial q(n',E)}{\partial E}\right)\cos\Big(\omega q(n',E)\Big)\Bigg\}dn',\end{aligned}$$

$$I_{311}(n,E) = \int_{n_0}^{n} \Bigg\{ \sqrt{2\Big(E-u(n)\Big)} \left[\left(\frac{\partial^2 q(n,E)}{\partial E^2} - \frac{\partial^2 q(n',E)}{\partial E^2} \right) \sin\Big(\omega q(n',E)\Big) - \omega \left(\frac{\partial q(n,E)}{\partial E} - \frac{\partial q(n',E)}{\partial E} \right)^2 \cos\Big(\omega q(n',E)\Big) \right] + \frac{1}{\sqrt{2\Big(E-u(n)\Big)}} \left(\frac{\partial q(n,E)}{\partial E} - \frac{\partial q(n',E)}{\partial E} \right) \sin\Big(\omega q(n',E)\Big) \Bigg\} (n')^2 \, dn',$$

$$I_{411}(n,E) = \int_{n_0}^{n} \Bigg\{ \sqrt{2\Big(E-u(n)\Big)} \left[\left(\frac{\partial^2 q(n,E)}{\partial E^2} - \frac{\partial^2 q(n',E)}{\partial E^2} \right) \cos\Big(\omega q(n',E)\Big) + \omega \left(\frac{\partial q(n,E)}{\partial E} - \frac{\partial q(n',E)}{\partial E} \right)^2 \sin\Big(\omega q(n',E)\Big) \right] + \frac{1}{\sqrt{2\Big(E-u(n)\Big)}} \left(\frac{\partial q(n,E)}{\partial E} - \frac{\partial q(n',E)}{\partial E} \right) \cos\Big(\omega q(n',E)\Big) \Bigg\} (n')^2 \, dn',$$

$$I_{112}(n,E) = \sqrt{2\Big(E-u(n)\Big)} \int_{n_0}^{n} \left(\frac{\partial q(n,E)}{\partial E} - \frac{\partial q(n',E)}{\partial E} \right) \sin\Big(\omega q(n',E)\Big) \, dn',$$

$$I_{212}(n,E) = \sqrt{2\Big(E-u(n)\Big)} \int_{n_0}^{n} \left(\frac{\partial q(n,E)}{\partial E} - \frac{\partial q(n',E)}{\partial E} \right) \cos\Big(\omega q(n',E)\Big) \, dn',$$

$$I_{312}(n,E) = \sqrt{2\Big(E-u(n)\Big)} \int_{n_0}^{n} \left(\frac{\partial q(n,E)}{\partial E} - \frac{\partial q(n',E)}{\partial E} \right) \sin\Big(\omega q(n',E)\Big) (n')^2 \, dn',$$

$$I_{412}(n,E) = \sqrt{2\Big(E-u(n)\Big)} \int_{n_0}^{n} \left(\frac{\partial q(n,E)}{\partial E} - \frac{\partial q(n',E)}{\partial E} \right) \cos\Big(\omega q(n',E)\Big) (n')^2 \, dn'.$$

The general solution of Eqs. (31), (32) contains only four unknown constants C_{10}, C_{20}, C_{11}, C_{21} and unknown parameters c and ωb. Equations for these unknowns follow from the normalization condition for the probability density $w(t,n,E)$, the equality to zero of $\langle n \rangle$, and the condition $m_3 = \langle n^3 \rangle = as(t) + b\dot{s}(t)$. These equations are

$$2 \int_{-0.25}^{\infty} \int_{\alpha(E)}^{n_2(E)} \frac{W_0(E)}{\sqrt{2\Big(E-u(n)\Big)}} \Big(w^{(e)}_{10,20}(n,E) + \epsilon w^{(e)}_{11,21}(n,E) + \epsilon^2 w^{(e)}_{12,22}(n,E) + \dots \Big) \, dn \, dE = 0,$$

$$2 \int_{-0.25}^{\infty} \int_{\alpha(E)}^{n_2(E)} \frac{nW_0(E)}{\sqrt{2\Big(E-u(n)\Big)}} \Big(w^{(o)}_{10,20}(n,E) + \epsilon w^{(o)}_{11,21}(n,E) + \epsilon^2 w^{(o)}_{12,22}(n,E) + \dots \Big) \, dn \, dE = 0,$$

$$2 \int_{-0.25}^{\infty} \int_{\alpha(E)}^{n_2(E)} \frac{n^3 W_0(E)}{\sqrt{2\Big(E-u(n)\Big)}} \Big(w^{(o)}_{10}(n,E) + \epsilon w^{(o)}_{11}(n,E) + \epsilon^2 w^{(o)}_{12}(n,E) + \dots \Big) \, dn \, dE = a, \tag{A6}$$

$$2 \int_{-0.25}^{\infty} \int_{\alpha(E)}^{n_2(E)} \frac{n^3 W_0(E)}{\sqrt{2\Big(E-u(n)\Big)}} \Big(w^{(o)}_{20}(n,E) + \epsilon w^{(o)}_{21}(n,E) + \epsilon^2 w^{(o)}_{22}(n,E) + \dots \Big) \, dn \, dE = \omega b,$$

where superscripts “e” or “o” point to the fact that either even or odd components must be calculated.

In the first approximation with respect to ϵ Eqs. (A6) become

$$\begin{aligned}
&\int\limits_{-0.25}^{\infty} W_0(E)\left[a_{11}C_{10}+a_{12}\,\omega b+\epsilon\left(c_{11}C_{20}+\frac{K}{2}\,a_{11}C_{11}+c_{12}(c+1)-3b_1\right)\right]\,dE=0,\\
&\int\limits_{-0.25}^{\infty} W_0(E)\left[a_{11}C_{20}-a_{12}(c+1)+3b_2-\epsilon\left(c_{11}C_{10}-\frac{K}{2}\,a_{11}C_{21}-c_{12}\,\omega b\right)\right]\,dE=0,\\
&\int\limits_{-0.25}^{\infty} W_0(E)\left[a_{21}C_{20}+a_{22}(c+1)-3b_3-\epsilon\left(c_{21}C_{10}-\frac{K}{2}\,a_{21}C_{21}-c_{22}\,\omega b\right)\right]\,dE=0,\\
&\int\limits_{-0.25}^{\infty} W_0(E)\left[-a_{21}C_{10}+a_{22}\,\omega b-\epsilon\left(c_{21}C_{20}+\frac{K}{2}\,a_{21}C_{11}+c_{22}(c+1)-3b_4\right)\right]\,dE=0,\\
&\int\limits_{-0.25}^{\infty} W_0(E)\left[a_{31}C_{20}+a_{32}(c+1)-3b_5-\epsilon\left(c_{31}C_{10}-\frac{K}{2}\,a_{31}C_{21}-c_{32}\,\omega b\right)\right]\,dE=a,\\
&\int\limits_{-0.25}^{\infty} W_0(E)\left[-a_{31}C_{10}+a_{32}\omega b-\epsilon\left(c_{31}C_{20}+\frac{K}{2}\,a_{31}C_{11}+c_{32}(c+1)-3b_6\right)\right]\,dE=\omega b,
\end{aligned}\tag{A7}$$

where

$$a_{11}=2\int\limits_{\alpha(E)}^{n_2(E)}\frac{\cos\Big(\omega q(n,E)\Big)}{\sqrt{2\Big(E-u(n)\Big)}}\,dn,\;\; a_{21}=2\int\limits_{\alpha(E)}^{n_2(E)}\frac{n\sin\Big(\omega q(n,E)\Big)}{\sqrt{2\Big(E-u(n)\Big)}}\,dn,\;\; a_{31}=2\int\limits_{\alpha(E)}^{n_2(E)}\frac{n^3\sin\Big(\omega q(n,E)\Big)}{\sqrt{2\Big(E-u(n)\Big)}}\,dn,$$

$$a_{12}=\frac{8\delta}{K}\int\limits_{\alpha(E)}^{n_2(E)}\frac{I_{20}(n,E)}{\sqrt{2\Big(E-u(n)\Big)}}\,dn,\;\; a_{22}=\frac{8\delta}{K}\int\limits_{\alpha(E)}^{n_2(E)}\frac{nI_{10}(n,E)}{\sqrt{2\Big(E-u(n)\Big)}}\,dn,\;\; a_{32}=\frac{8\delta}{K}\int\limits_{\alpha(E)}^{n_2(E)}\frac{n^3I_{10}(n,E)}{\sqrt{2\Big(E-u(n)\Big)}}\,dn,$$

$$b_2=\frac{8\delta}{K}\int\limits_{\alpha(E)}^{n_2(E)}\frac{I_{40}(n,E)}{\sqrt{2\Big(E-u(n)\Big)}}\,dn,\;\; b_3=\frac{8\delta}{K}\int\limits_{\alpha(E)}^{n_2(E)}\frac{nI_{30}(n,E)}{\sqrt{2\Big(E-u(n)\Big)}}\,dn,\;\; b_5=\frac{8\delta}{K}\int\limits_{\alpha(E)}^{n_2(E)}\frac{n^3I_{30}(n,E)}{\sqrt{2\Big(E-u(n)\Big)}}\,dn,$$

$$c_{11}=\omega K\int\limits_{\alpha(E)}^{n_2(E)}\left[\frac{\cos\Big(\omega q(n,E)\Big)}{\sqrt{2\Big(E-u(n)\Big)}}\left(I_{21}(n,E)-\frac{4\delta}{K}\,I_{31}(n,E)\right)-\frac{\omega\sin\Big(\omega q(n,E)\Big)}{\sqrt{2\Big(E-u(n)\Big)}}\,I_{11}(n,E)\right]dn,$$

$$c_{21}=\omega K\int\limits_{\alpha(E)}^{n_2(E)}\left[\frac{\sin\Big(\omega q(n,E)\Big)}{\sqrt{2\Big(E-u(n)\Big)}}\left(I_{21}(n,E)-\frac{4\delta}{K}\,I_{31}(n,E)\right)+\frac{\omega\cos\Big(\omega q(n,E)\Big)}{\sqrt{2\Big(E-u(n)\Big)}}\,I_{11}(n,E)\right]n\,dn,$$

$$c_{31}=\omega K\int\limits_{\alpha(E)}^{n_2(E)}\left[\frac{\sin\Big(\omega q(n,E)\Big)}{\sqrt{2\Big(E-u(n)\Big)}}\left(I_{21}(n,E)-\frac{4\delta}{K}\,I_{31}(n,E)\right)+\frac{\omega\cos\Big(\omega q(n,E)\Big)}{\sqrt{2\Big(E-u(n)\Big)}}\,I_{11}(n,E)\right]n^3\,dn,$$

$$c_{12}=4\omega\delta\int\limits_{\alpha(E)}^{n_2(E)}\left(\frac{\cos\Big(\omega q(n,E)\Big)}{\sqrt{2\Big(E-u(n)\Big)}}\,J_1(n,E)-\frac{\sin\Big(\omega q(n,E)\Big)}{\sqrt{2\Big(E-u(n)\Big)}}\,J_2(n,E)\right)dn,$$

$$c_{22} = 4\omega\delta \int\limits_{\alpha(E)}^{n_2(E)} \left(\frac{\cos\Big(\omega q(n,E)\Big)}{\sqrt{2\Big(E-u(n)\Big)}} J_2(n,E) + \frac{\sin\Big(\omega q(n,E)\Big)}{\sqrt{2\Big(E-u(n)\Big)}} J_1(n,E) \right) n\,dn,$$

$$c_{32} = 4\omega\delta \int\limits_{\alpha(E)}^{n_2(E)} \left(\frac{\cos\Big(\omega q(n,E)\Big)}{\sqrt{2\Big(E-u(n)\Big)}} J_2(n,E) + \frac{\sin\Big(\omega q(n,E)\Big)}{\sqrt{2\Big(E-u(n)\Big)}} J_1(n,E) \right) n^3\,dn,$$

$$b_1 = 4\omega\delta \int\limits_{\alpha(E)}^{n_2(E)} \left(\frac{\cos\Big(\omega q(n,E)\Big)}{\sqrt{2\Big(E-u(n)\Big)}} J_3(n,E) - \frac{\sin\Big(\omega q(n,E)\Big)}{\sqrt{2\Big(E-u(n)\Big)}} J_4(n,E) \right) dn,$$

$$b_4 = 4\omega\delta \int\limits_{\alpha(E)}^{n_2(E)} \left(\frac{\cos\Big(\omega q(n,E)\Big)}{\sqrt{2\Big(E-u(n)\Big)}} J_4(n,E) + \frac{\sin\Big(\omega q(n,E)\Big)}{\sqrt{2\Big(E-u(n)\Big)}} J_3(n,E) \right) n\,dn,$$

$$b_6 = 4\omega\delta \int\limits_{\alpha(E)}^{n_2(E)} \left(\frac{\cos\Big(\omega q(n,E)\Big)}{\sqrt{2\Big(E-u(n)\Big)}} J_4(n,E) + \frac{\sin\Big(\omega q(n,E)\Big)}{\sqrt{2\Big(E-u(n)\Big)}} J_3(n,E) \right) n^3\,dn.$$

3. Second order and higher approximations

The expressions for $B_{1j}(n,E)$ and $B_{2j}(n,E)$ in the second and higher approximations are more cumbersome than those above, so we will not write them explicitly. Note that, starting with the second approximation, we should take into account only partial solutions of the corresponding inhomogeneous equations. In the second approximation Eqs. (A6) are transformed to equations similar to (A7) but more complicated.

[1] R. Benzi, A. Sutera, and A. Vulpiani, J. Phys. A: Math. Gen. **14**, L453 (1981).
[2] C. Nicolis, Tellus **34**, 1 (1982).
[3] R. Benzi, G. Parisi, A. Sutera, and A. Vulpiani, Tellus **34**, 10 (1982).
[4] M. I. Dykman, D. G. Luchinsky, R. Mannella, P. V. E. McClintock, N. D. Stein, and N. G. Stocks, Nuovo Cimento D **17**, 661 (1995).
[5] L. Gammaitoni, P. Hänggi, P. Jung, and F. Marchesoni, Rev. Mod. Phys. **70**, 223 (1998).
[6] V. S. Anishchenko, A. B. Neiman, F. Moss, and L. Schimansky-Geier, Soviet Phys. – Uspekhi Fiz. Nauk. **39**, 7 (1999).
[7] P. S. Landa, *Regular and Chaotic Oscillations* (Springer-Verlag, Berlin, 2001).
[8] I. I. Blekhman, *Vibrational Mechanics.* (World Scientific, Singapore, 2000)
[9] P. S. Landa, and P. V. E. McClintockm J. Phys. A **33**, L433 (2000).
[10] M. Borromeo, and F. Marchesoni, Phys. Rev. Lett. **99**, 150605 (2007).
[11] S. Fauve and F. Heslot, Phys. Lett. A **97**, 5 (1983).
[12] R. N. Mantegna, and B. Spagnolo, Phys. Rev. E **49**, R1792 (1994).
[13] R. N. Mantegna, B. Spagnolo, and M. Trapanese, Phys. Rev. E **63**, 011101 (2001).
[14] B. McNamara, K. Wiesenfeld, and R. Roy, Phys. Rev. Lett. **60**, 2626 (1988).
[15] P. S. Landa and V. G. Ushakov, Pis'ma JETF **86**, 000 (2007).
[16] M. I. Dykman, R. Mannella, P. V. E. McClintock, and N. G. Stocks, Phys. Rev. Lett. **65**, 2606 (1990).
[17] P. Debye, *Polar Molecules* (Dover publications, Inc., New York, 1929).
[18] M. I. Dykman, R. Mannella, P. V. E. McClintock, and N. G. Stocks, Phys. Rev. Lett. **68**, 2985 (1992).
[19] M. I. Dykman, R. Mannella, P. V. E. McClintock, and N. G. Stocks, Phys. Rev. Lett. **70**, 874 (1993).
[20] N. G. Stocks, N. D. Stein, and P. V. E. McClintock, J. Phys. A: Math. Gen. **26**, L385 (1993).
[21] M. I. Dykman, D. G. Luchinsky, R. Mannella, P. V. E. McClintock, N. D. Stein, and N. G. Stocks, Sov. Phys. JETP Lett. **58**, 150 (1993).
[22] M. I. Dykman, D. G. Luchinsky, R. Mannella, P. V. E. McClintock, N. D. Stein, and N. G. Stocks, Phys. Rev. E **49**, 1198 (1994).
[23] P. S. Landa, Doklady Physics **49**, 706 (2004).
[24] P. Landa, V. Ushakov, and J. Kurths, Chaos, Solitons & Fractals **30**, 574 (2006).
[25] P. S. Landa, Y. I. Neimark, and P. V. E. McClintock, J. Stat. Phys. **125**, 593 (2006).
[26] L. Gammaitoni, F. Marchesoni, E. Menichella-Saetta, and S. Santucci, Phys. Rev. Lett. **62**, 349 (1989).
[27] M. I. Dykman, P. V. E. McClintock, R. Mannella, and

N. G. Stocks, Pis'ma Zh. Eksp. Teor. Fiz. [JETP lett.] **52**, 780 (1990).

[28] L. Alfonsi, L. Gammaitoni, S. Santucci, and A. R. Bulsara, Phys. Rev. E **62**, 299 (2000).

[29] Y.-M. Kang, J.-X. Xu, and Y. Xie, Phys. Rev. E **68**, 036123 (2003).

[30] D. Valenti, L. Schimansky-Geier, X. Sailer, and B. Spagnolo, Eur. Phys. J. B **50**, 199 (2006).

[31] M. I. Dykman, D. G. Luchinsky, R. Mannella, P. V. E. McClintock, N. D. Stein, and N. G. Stocks, J. Stat. Phys. **70**, 479 (1993).

[32] Note that this definition is based on that applied to linear systems, whereas the signal-to-noise ratio for a nonlinear system is ambiguously determined.

[33] The power spectrum $P(\Omega)$ was calculated by the periodogram method with a rectangular time window, and signal amplitude spectrum $F(\Omega)$ was calculated by the base-2 fast Fourier transform: $P(\Omega_j) = \frac{1}{N}\sum_{k=1}^{N} F_k^2(\Omega_j)$, $N = 300$ is the number of periodograms. The length of the periodogram was equal to 65536 points and the time sampling interval was $\Delta = 2\pi/(\omega 2^k)$, where $k = 4$. Given the last condition, the leakage effect is absent for a periodic signal of frequency ω, i.e. one frequency bin $\Delta\Omega$ contains all the power of the harmonic signal. To avoid aliasing, a low-frequency linear filter with cut-off frequency 5ω was used.

[34] R. L. Stratonovich, Vestnik MGU No. 4 pp. 99–102 (1960).

[35] R. L. Stratonovich, *Topics in the Theory of Random Noise*, vols. 1 & 2 (Gordon and Breach, New York, 1963, 1967).

[36] M. Abramowitz and I. Stegun, *Handbook of Mathematical Functions* (Dover, New York, 1965).